文章编号：1001-9014(2025)05-0631-10

DOI:10.11972/j.issn.1001-9014.2025.05.001

NIR-II quantum dot-labeled exosomes' imaging in treatment of ischemic peripheral nerve injury

OGURA Shingo[1,3], SHAO Ke-Meng[1], ZHANG Xiao[2], LI Hui-Zhu[2], FENG Si-Jia[2], WANG Yue-Ming[1], CHEN Jun[2], WU De-Hua[3*], WO Yan[1*]

(1. Department of Anatomy and Physiology, Shanghai Jiao Tong University School of Medicine, Shanghai 200025, China;
2. Department of Orthopedic Sports Medicine, Huashan Hospital Affiliated to Fudan University, Shanghai 200040, China;
3. Department of Anesthesia, Songjiang Research Institute, Songjiang Hospital Affiliated to Shanghai Jiao Tong University School of Medicine, Shanghai 200025, China)

Abstract: Ischemia is a significant factor affecting the repair of peripheral nerve injuries, while exosomes have been shown to promote angiogenesis. To further investigate the detailed processes and efficacy of exosome therapy for ischemic peripheral nerve injuries, this study utilized glucose-modified near-infrared-II (NIR-II) quantum dots (QDs) to label adipose-derived stem cell exosomes (QDs-ADSC-Exos), enabling long-term in vivo NIR-II imaging of exosome treatment for ischemic peripheral nerve damage. Experimental results confirmed that QDs can be used for non-invasive in vitro labeling of exosomes, with QDs-ADSC-Exos exhibiting strong fluorescence signals in the NIR-II window and demonstrating favorable NIR-II imaging characteristics in vivo. Notably, QDs-ADSC-Exos showed accumulation at the site of nerve injury in cases of ischemic peripheral nerve damage. Functional neurological assessments indicated that QDs-ADSC-Exos effectively promoted neural regeneration. This study highlights the potential of exosomes in treating ischemic peripheral nerve injuries and elucidates the spatio-temporal characteristics of exosome therapy, providing objective evidence for the further optimization of exosome-based treatment protocols.

Key words: NIR-II imaging, quantum dots, exosomes, peripheral nerve injury, vascular injury

近红外二区量子点标记外泌体治疗伴缺血周围神经损伤过程的体内成像研究

小仓心吾[1,3], 邵珂萌[1], 张 晓[2], 李惠珠[2], 冯思嘉[2], 王月明[1], 陈 俊[2], 吴德华[3*], 沃 雁[1*]

(1. 上海交通大学医学院 解剖学与生理学系,上海 200025;
2. 复旦大学运动医学研究所 复旦大学附属华山医院运动医学科,上海 200040;
3. 上海交通大学医学院附属松江医院 麻醉科,上海 200025)

摘要:缺血是影响周围神经损伤修复的重要因素,而外泌体被证实具有促血管再生作用。为了进一步研究外泌体治疗伴缺血周围神经损伤的细节过程与疗效,本文利用葡萄糖修饰近红外二区量子点标记脂肪干细胞来源外泌体(QDs-ADSC-Exos),实现外泌体治疗伴缺血周围神经损伤的活体近红外二区(NIR-II)长时程成像。实验结果证实量子点可用于体外无创标记外泌体,QDs-ADSC-Exos在NIR-II区间下显示出高强度荧光信号,在体内具备良好的NIR-II活体成像特性;QDs-ADSC-Exos在伴缺血周围神经损伤中表现为在神经损伤局部的聚集;神经功能学评估果表明,QDs-ADSC-Exos能促进有效神经功能再生。本研究证明外泌体在伴缺血周围神经损伤治疗中的潜力,也发现外泌体治疗伴缺血周围神经损伤的时空变化特征,为了进一步优化外泌体治

Received date: 2024-11-03, **revised date**: 2025-03-24 **收稿日期**:2024-11-03,**修回日期**:2025-03-24

Foundation items: Supported by the National Natural Science Foundation of China (82371373, W2412120); the Shanghai Natural Science Foundation (21ZR1436100).

Biography: OGURA Shingo (1998-), male, Shanghai, Master. Research area involves peripheral nerve injury and repair. Email: ogurashingow@126.com

* **Corresponding authors**: E-mail: wudehua74@163.com; woyansh@163.com

疗方案提供了客观依据。

关 键 词:近红外二区成像;量子点;外泌体;周围神经损伤;血管损伤

中图分类号:R3 **文献标识码**:A

Introduction

Peripheral nerve injury (PNI) is a common clinical traumatic condition that leads to functional impairments, such as sensory deficits, loss of motor function, and pain, severely impacting patients' quality of life[1]. While peripheral nerves possess intrinsic self-repair capabilities, clinical cases often involve nerve damage coupled with ischemia due to accompanying vascular injury[2]. Although peripheral nerves are supported by a complex interconnected vascular network that provides some compensatory mechanisms, extensive damage can still lead to ischemia, impeding nerve regeneration[3]. Current research on PNI treatment primarily focuses on isolated nerve injury models, with limited studies addressing the evaluation of nerve-vascular complex injury models.

Recent advances in neurobiology and regenerative medicine have opened new avenues for PNI treatment, particularly through cell therapies and the application of biomaterials[4-5]. Among these, exosomes (Exos) have attracted increasing attention due to their significant role in regulating nerve regeneration and tissue repair[6]. Exosomes, extracellular vesicles (EVs) ranging from 50 to 150 nm in diameter, are secreted by cells and carry proteins, lipids, RNA, and other bioactive molecules that facilitate various biological processes, including cell proliferation, differentiation, immune modulation, and tissue repair[7]. In the context of PNI, exosomes promote nerve regeneration by enhancing neuronal survival, axonal regeneration, and modulating immune responses[8].

Exosomes can be derived from multiple cell types, including mesenchymal stem cells (MSCs), neural stem cells (NSCs), and induced pluripotent stem cells (iPSCs)[9]. Among these, MSC-derived exosomes (MSC-Exos) have shown remarkable efficacy in promoting neuronal repair, reducing inflammation post-nerve injury, and enhancing angiogenesis[10].

Although exosomes have shown significant bioactivity in vitro, monitoring their behavior and therapeutic effects in vivo remains a challenge. Due to their nanoscale size, exosomes are often cleared by the immune system or rapidly metabolized. Therefore, improving their targeting, stability, and persistence in vivo is crucial for their successful application. Developing real-time monitoring methods for exosomes in vivo is crucial for guiding their use in treating nerve-vascular complex injuries.

In recent years, near-infrared II (NIR-II) imaging technology has shown great promise in tracking stem cells and EVs like exosomes in vivo[11-12]. Compared to traditional visible and near-infrared I (NIR-I) imaging, the NIR-II wavelength range (1000-1700 nm) offers stronger tissue penetration and higher signal-to-noise ratio, allowing clearer and more accurate imaging of deep tissues[13]. Quantum dots (QDs), as one of the markers for NIR-II imaging, have become widely used as fluorescent probes in biological imaging due to their superior optical properties, such as high brightness, stable fluorescence signals, and tunable emission wavelengths[14]. By labeling stem cells or exosomes with quantum dots, researchers can monitor their distribution, migration, and accumulation in vivo, thereby providing insights into their roles in tissue repair and regeneration. In the field of peripheral nerve injuries, the combination of NIR-II imaging with quantum dot labeling enhances imaging sensitivity and resolution, providing valuable imaging support for studying the targeting, mechanisms, and therapeutic efficacy of stem cells and exosomes.

In this study, glucose-crosslinked QDs were used to label exosomes derived from adipose-derived stem cells (ADSC-Exos). Ribonuclease-A (RNase-A) encapsulated PbS quantum dots (PbS QDs) were labeled on ADSC-Exos, and the imaging properties and stability of QD-labeled exosomes (QDs-ADSC-Exos) were studied in vitro and in vivo using an NIR-II imaging system. The approach was applied to a rat model with femoral artery and vein ligation, accompanied by femoral nerve injury to track exosome distribution in real-time. The nerve regeneration-promoting effects of the exosomes were evaluated using electrophysiological, behavioral, and histological analyses. This study aimed to investigate the spatiotemporal characteristics and therapeutic efficacy of exosomes in treating nerve-vascular complex injuries, providing new evidence for the clinical application of exosomes.

1 Experiments

1.1 Reagents and materials

Lead acetate trihydrate ($Pb(OAc)_2 \cdot 3H_2O$, 99.9%, J&K Scientific), sodium sulfide nonahydrate ($Na_2S \cdot 9H_2O$, ≥98.0%, J&K Scientific), bovine pancreatic RNase-A (MW: 13.7 kDa, >70 U/mg, Yeason), sodium hydroxide (NaOH, 95%, Macklin), N-hydroxysuccinimide (NHS, 98%, Adamas Life), 1-Ethyl-3-(3-dimethylaminopropyl) carbon diamine hydrochloride (EDC, 97%+, Adamas Life), D-(+)-glucosamine hydrochloride (2-GF, 98%, Adamas Life), DMEM/F12 (Adamas Life), penicillin-streptomycin solution (100×) (Adamas Life), fetal bovine serum (Adamas Life), trypsin-EDTA (0.25% Trypsin-0.93mM EDTA, Adamas Life), collagenase type I (Adamas Life), 1× PBS (pH=7.4, Adamas Life), paraformaldehyde (4% PFA, Adamas Life), isoflurane (RWD), etc.

1.2 Animals

Female SD rats(6-8 weeks), SD rats(7 days), and female nude mice (6-8 weeks) were purchased from Shanghai Lingchang Biotechnology Co., Ltd. (Shanghai, China). This work received the approval of ethics by the Animal Care and Use Committee of Shanghai Jiao

Tong University School of Medicine, approval number: JUMC2023-067-A-A.

1.3 Instrumentation

A microwave reactor (Discover, CEM) was used for PbS QDs synthesis; 10 kDa ultrafiltration tubes (Millipore) were used for PbS QDs and ADSC-Exos extraction; an 808 nm semiconductor laser system provided illumination with an excitation light power of 100 mW/cm^2; a 1100 nm long-pass filter was used to filter emission light, which was collimated by a 50 mm NIR-II lens (Goldeye G-130 TEC1, Allied Vision). Fluorescence was detected using an InGaAs camera (NIRvana 640, Teledyne Princeton Instruments) located vertically above the sample on the working stage; transmission electron microscopy (HT7700- HITACHI) was used to observe the morphology of PbS QDs, ADSC-Exos, and QDs-ADSC-Exos; nanoparticle tracking analysis (NTA, Zeta-View PMX 110, Particle Metrix) was used to measure particle size distribution and zeta potential; and a PowerLab 8/35 data acquisition system (ADInstruments) was used to detect the compound muscle action potential (CMAP) of quadriceps.

1.4 Extraction and culture of ADSCs

Inguinal fat pad tissues from 7-day-old SD rats were excised, vessels and capsule removed, and the tissues cut into 1x1x1 mm^3 pieces. The tissue fragments were mixed with 0.15% type I collagenase at a 1:2 ratio, digested in a 37°C water bath for 1 hour, with inversion every 20 minutes. After digestion, the solution was centrifuged at 1 500g for 8 minutes, the upper fat and digestion fluid were discarded, and the precipitate resuspended in PBS and transferred to a new centrifuge tube. The solution was again centrifuged at 1 500g for 8 minutes, and the supernatant removed. The cells were resuspended in complete DMEM/F12 medium containing 10% FBS and 1% penicillin/streptomycin, filtered through 100 μm and 70 μm sieves to remove residual tissue fragments, and cultured in T25 flasks. The medium was replaced after 24 hours and subsequently every two days. When cell density reached 70-80%, cells were digested with 0.25% trypsin-EDTA solution and passaged at a 1:3 ratio.

1.5 ADSC-Exos extraction and identification

When the P3 adipose stem cells reached 90% confluence, the supernatant was discarded, and the cells washed twice with PBS. Serum-free DMEM/F12 was added for 48-hour culture. The collected supernatant was centrifuged at 3 500 g for 15 minutes to remove dead cells, filtered through a 0.22 μm filter, and ultrafiltrated at 3 500 g to obtain the exosome suspension. The ultrafiltration tube was washed with PBS and centrifuged again at 3 500 g until the inner liquid was colorless. Exosome protein concentration was quantified using BCA, morphology was observed with TEM, and size and zeta potential were measured by particle size analysis.

1.6 PbS QDs synthesis

PbS QDs were synthesized using a modified method based on Dejian Zhou's protocol[15]. $Pb(OAc)_2 \cdot 3H_2O$ (10 mM) and RNase-A (50 mg/mL) solutions were mixed in a reaction tube. The mixture (1 mL) was combined with 50 μL of 1 M NaOH to adjust pH to 9-11. Then, 50 μL of 10 mM Na_2S solution was added, mixed, and reacted in a microwave reactor at 70 °C for 30 seconds. After cooling to room temperature, the solution was purified using a 10 kDa ultrafiltration tube, and the prepared PbS QDs were stored at 4°C.

1.7 PbS QDs labeling of ADSC-Exos

The pH of the PbS QDs solution was adjusted to 5-6. 0.24 mg EDC and 0.24 mg NHS were added to 1 mL of PbS QDs solution, and the mixture was shaken at room temperature for 40 minutes. Then, 0.175 mg of 2-GF was added and incubated at 4 °C overnight. The unbound impurities were removed using an ultrafiltration tube. The ADSC-Exos were incubated with glucose-cross-linked PbS QDs at 4 °C overnight to prepare PbS QDs-labeled ADSC-Exos (QDs-ADSC-Exos).

1.8 Preparation of experimental animal models

After one week of adaptive feeding, healthy female rats were anesthetized via inhalation of isoflurane and positioned supine. The left femoral artery and vein were exposed, and the vascular sheath was separated to free the femoral vein. The femoral artery and vein were ligated with 6-0 sutures at the groin. Using the bifurcation of the femoral nerve as a reference point, the femoral nerve trunk was clamped with a spring-loaded forceps 3 mm proximally for 30 seconds to induce a 2 mm nerve crush injury. Immediately following the nerve crush, 5 μl of QDs-ADSCs-Exosomes was injected into the proximal site of the nerve injury, while the control group received 5 μl of Phosphate buffered saline (PBS). After the injection, the incision was sutured, and the rats were regularly cared for after ethanol disinfection.

1.9 In vivo NIR-II imaging

Nude mice were anesthetized with isoflurane and fixed in a prone position. Different concentrations of QDs-ADSC-Exos (0.5 mg/mL, 0.1 mg/mL, 0.05 mg/mL) and PbS QDs were subcutaneously injected. NIR-II imaging was performed at 0, 1, 2, 3, 5, and 7 days post-injection. In a rat ischemic femoral nerve injury model, 5 μL of 0.5 mg/mL QDs-ADSC-Exos was injected, and imaging was conducted immediately, then at 6, 12, 24, 48, and 72 hours. The PL intensity was measured from the site of the injury of collected NIR-II images using Fiji

1.10 Electromyography

Under isoflurane anesthesia, the left femoral nerve and quadriceps muscle were exposed. A stimulating electrode was placed on the proximal end of the injured femoral nerve, while a recording needle electrode was inserted into the quadriceps muscle, and a ground electrode was connected to the rat's tail. Electrical stimulation was set at 1.5 mA, and the electrical signals from the quadriceps muscle were recorded to measure the amplitude of the muscle's response.

1.11 Behavioral tests

Behavioral tests were conducted following the evaluation methods for femoral nerve motor function as described by A. Irintchev et al[16]. All behavior experiments

were conducted in a blinded fashion in a quiet room (temperature (22 ± 1) °C). Prior to surgery, each rat was placed at one end of a 1.5 m long, 15 cm wide, and 5 cm thick wooden board, with a cage at the opposite end to encourage movement. The rats were trained to walk toward the cage, and the step length ratio (SLR) and footbase angle (FBA) during locomotion were recorded one day before the surgery, and again at days 1 and 28 post-injection. The recovery index (RI) was calculated to evaluate the restoration of femoral nerve motor function using the following formula:

$$RI = \frac{Y_{28} - Y_1}{Y_0 - Y_1} \times 100\%, \quad (1)$$

Y_0 is the value recorded one day before surgery, Y_1 is the value on day 1 post-injection, and Y_{28} is the value on day 28 post-injection.

1.12 Statistical analysis

ImageJ was used to analyze imaging data. OriginPro 2024 for statistical processing. All numerical data were presented as mean ± SD and analyzed using Student's t-test. $P<0.05$ was considered statistically significant.

2 Results and discussions

2.1 Characterization of PbS QDs and QDs-ADSC-Exos

Synthesized PbS QDs appeared as well-dispersed particles under TEM, presenting as high-contrast black dots with a near-spherical shape and an approximate diameter of 10 nm. High-resolution images showed distinct and regularly arranged lattice fringes (Figure 1(a)). Particle size analysis revealed an average diameter of 13 nm, slightly larger than observed under TEM, possibly due to some aggregation in the solution (Figure 1(b)). The average zeta potential was found to be -0.13 mV (Figure 1(c)).

Glucose was encapsulated onto PbS QDs through glucose modification, forming QDs-Glu complexes, which were then incubated with exosomes to label the quantum dots on the exosomes. Transmission electron microscopy revealed that QDs-ADSC-Exos retained a discoid concave structure with a diameter of approximately 100 nm. Compared to ADSC-Exos alone, multiple black particles were observed attached to the surface of QDs-ADSC-Exos (Figure 2(a), (d)). Particle size analysis indicated that the average diameter of QDs-ADSC-Exos was 114.7 nm, slightly larger than that of ADSC-Exos (108.2 nm), likely due to the surface modification by PbS QDs on ADSC-Exos and minor aggregation of ADSC-Exos in the cross-linking agent solution (Figure 2(b), (e)). The average Zeta potential of QDs-ADSC-Exos was measured at -1.64 mV, suggesting interactions between PbS QDs and the ADSC-Exos surface, altering the Zeta potential from -35.36 mV of ADSC-Exos alone (Figure 2(c), (f)).

The QDs-Glu complex was formed by encapsulating the QDs with glucose modification, and then incubated with the exosomes to label the ADSC-Exos. The optical properties of the QDs-ADSC-Exos complexes were analyzed using an NIR-II imaging device to capture variations in fluorescence intensity at different exposure times. Under 808 nm excitation light and with an 1100 nm long-pass filter, the photoluminescence (PL) intensity of QDs-ADSC-Exos increased with longer exposure times, approaching maximum fluorescence intensity at 50 ms exposure (Figure 3). The results indicate that QDs-ADSC-Exos exhibit high-intensity fluorescence imaging in the NIR-II range.

2.2 In vivo imaging of QDs-ADSC-Exos

To verify the in vivo imaging stability and sensitivity of QDs-ADSC-Exos, three concentrations (0.5 mg/mL, 0.1 mg/mL, 0.05 mg/mL) and PbS QDs as control were subcutaneously injected into the back of nude mice. NIR-II imaging was performed at 0, 1, 2, 3, 5, and 7 days post-injection. As shown in Fig. 4, immediately after subcutaneous injection, four points (I, II, III, IV) exhibited varying fluorescence intensities, and the intensity at points I, II, and III was linearly correlated with the exosome concentration (Figure 4(d)). Analysis of fluorescence area and intensity over time revealed a gradual decrease at all points, with signals persisting at points I, II, and IV until day 7 (Figure 4(b), (c)). These results indicate that quantum dot-labeled exosomes enable stable in vivo imaging.

Specifically, the concentration of 0.5 mg/mL dem-

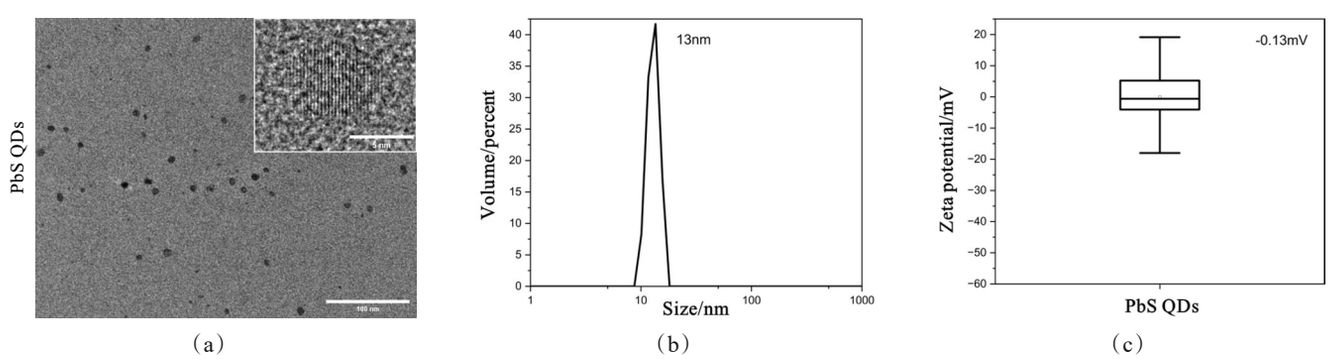

(a) (b) (c)

Fig. 1 Characterization of PbS QDs: (a) the TEM image(scale bar = 100 nm; inset scale bar = 5 nm); (b) particle size and distribution; (c) average zeta potential of PbS QDs

图1 PbS QDs材料表征:(a)透射电镜图像(标尺=100nm,右上方小图中标尺=5nm);(b)粒径大小和分布;(c)平均Zeta电位

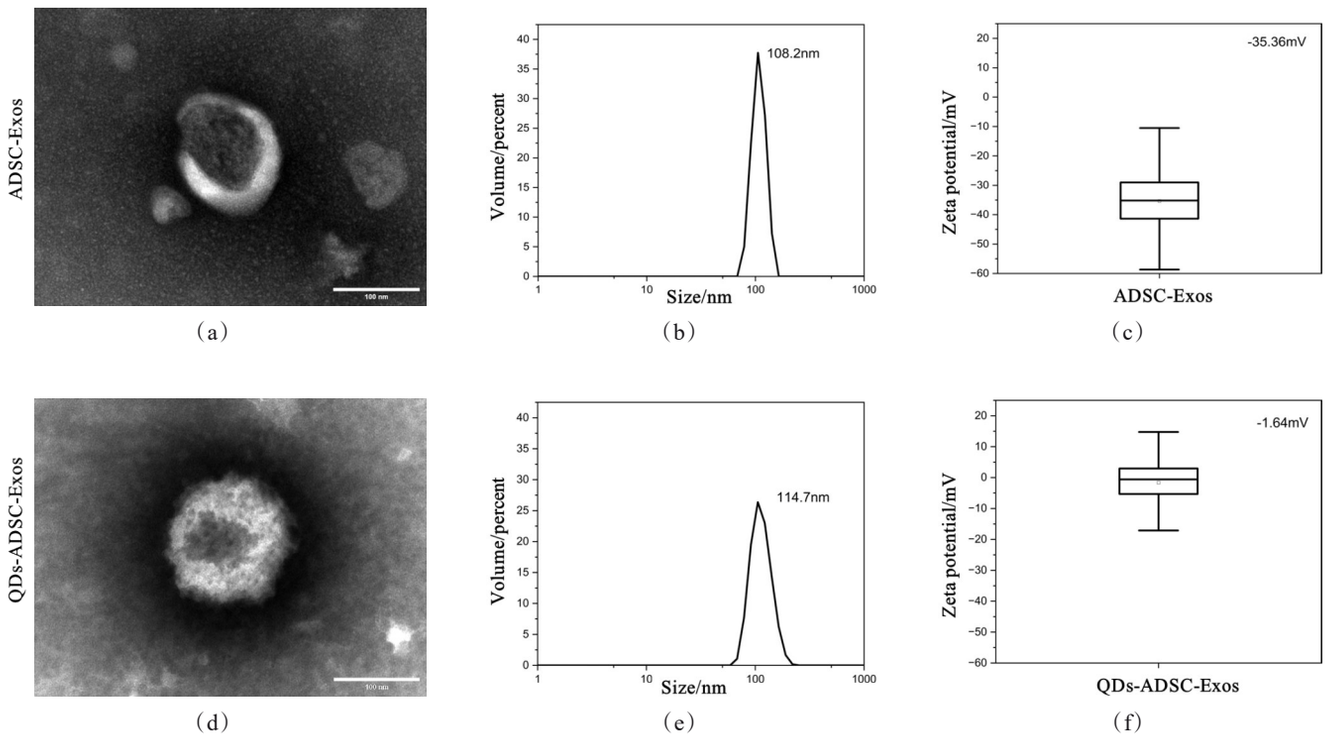

Fig. 2 Characterization of ADSC-Exos and QDs-ADSC-Exos: (a) the TEM image(scale bar = 100 nm); (b) particle size and distribution; (c) average zeta potential of ADSC-Exos; (d) the TEM image(scale bar = 100 nm); (e) particle size and distribution; (f) average zeta potential of QDs-ADSC-Exos

图 2 ADSC-Exos 及 QDs-ADSC-Exos 材料表征：ADSC-Exos 的(a)透射电镜图像(标尺=100nm)；(b)粒径大小和分布；(c)平均 Zeta 电位；QDs-ADSC-Exos 的(d)透射电镜形态(标尺=100nm)；(e)粒径大小和分布；(f)平均 Zeta 电位

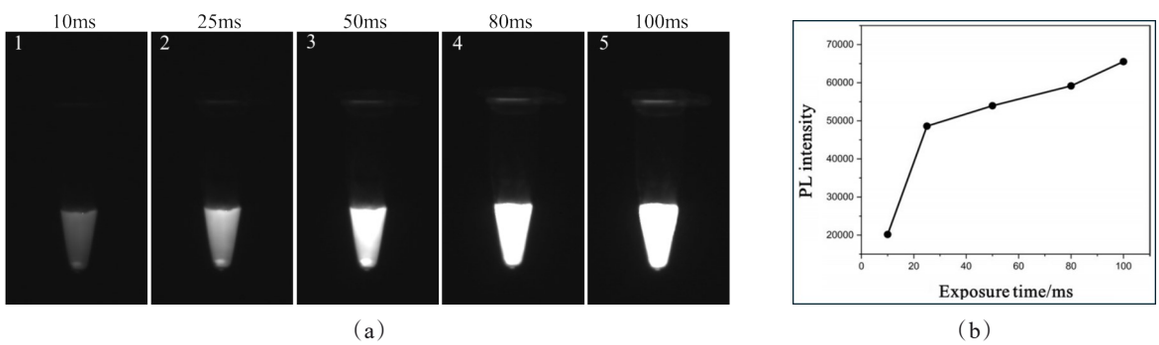

Fig. 3 Optical property of the QDs-ADSC-Exos: (a) QDs-ADSC-Exos with NIR-II fluorescence imaging at different exposure times (10 ms, 25 ms, 50 ms, 80 ms, 100 ms, λex: 808 nm); (b) PL intensity in NIR-II imaging across different exposure times

图 3 QDs-ADSC-Exos 光学特征：QDs-ADSC-Exos(a)在 10 ms、25 ms、50 ms、80 ms、100 ms 的曝光时间下的 NIR-II 区荧光成像(λex: 808 nm)；(b)不同曝光时间下 NIR-II 成像的 PL 荧光强度

onstrated the highest fluorescence signals with the longest duration, indicating that QDs-ADSC-Exos were most effectively detected at this concentration using the NIR-II imaging system. Both PL intensity and fluorescence area analysis revealed that QDs-ADSC-Exos at 0.5 mg/mL exhibited a gradual decrease in signal, suggesting prolonged retention at the injection site with stable fluorescence maintained throughout the 7-day observation period (Figure 4(b), (c)). Consequently, 0.5 mg/mL was identified as the optimal concentration and was selected for subsequent in vivo experiments.

To observe the spatiotemporal dynamics of QDs-ADSC-Exos in ischemic peripheral nerve injury, we established a rat model with femoral artery and vein ligation combined with femoral nerve clamp injury. Immediately after injury, 5 μl of 0.5 mg/ml QDs-ADSC-Exos was injected subepineurally at the proximal end of the injured femoral nerve. Near-infrared (NIR) fluorescence imaging was conducted at 0 h, 6 h, 12 h, 24 h, 48 h, and 72 h post-injection. As shown in Fig. 5(a1)-(a2), a strong

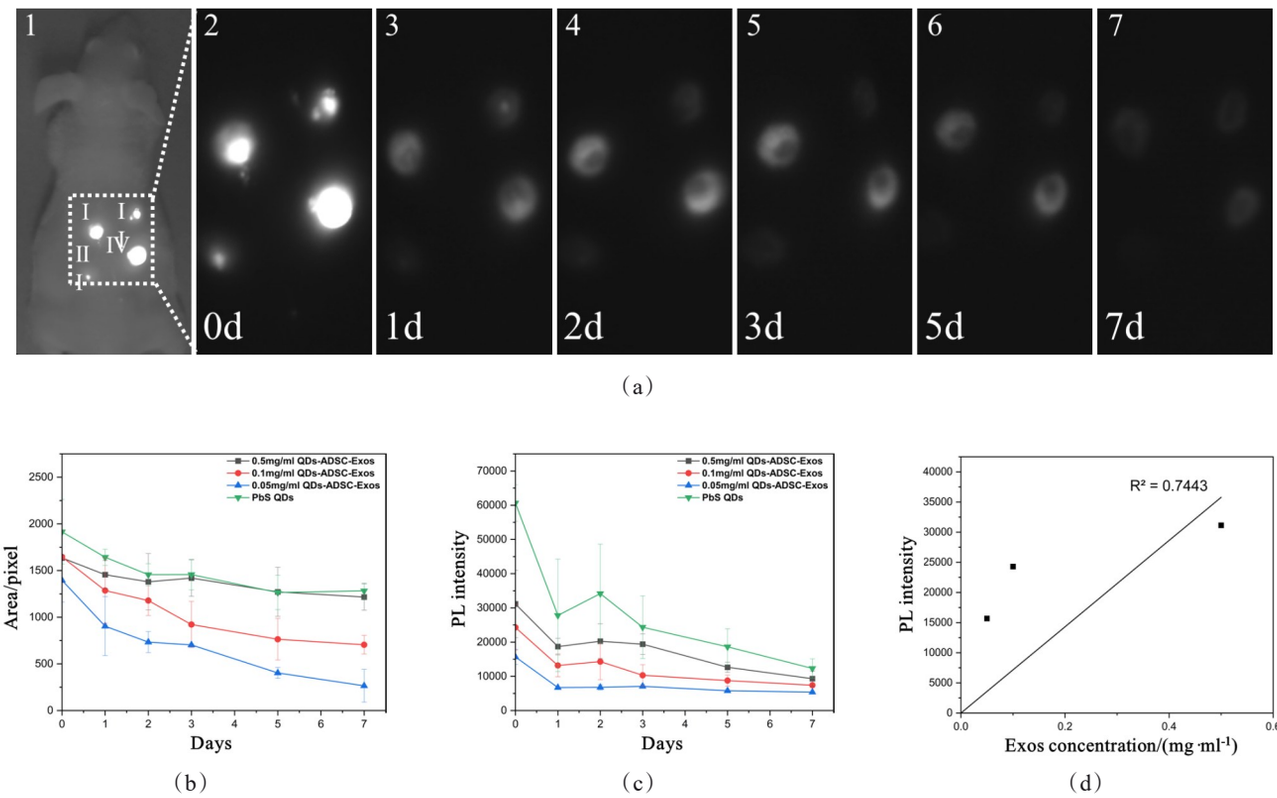

Fig. 4 Validation of the sensitivity and stability of QDs-ADSC-Exos in vivo: (a1-a7) NIR-II fluorescence imaging of QDs-ADSC-Exos and PbS QDs injected subcutaneously into the dorsal region of nude mice at 0, 1, 2, 3, 5, and 7 days post-injection. Regions I, II, III, and IV correspond to injection sites of 0.5 mg/ml, 0.1 mg/ml, 0.05 mg/ml exosomes, and PbS QDs, respectively (λex: 808 nm, exposure time: 300 ms); (b) longitudinal comparison of the fluorescence area at different injection sites; (c) longitudinal comparison of PL intensity at different injection sites; (d) the linear correlation result between fluorescence intensity and exosome concentration at the injection site on day 0

图4 QDs-ADSC-Exos体内敏感性和稳定性验证:(a1-a7)QDs-ADSC-Exos和PbS QDs注射到裸鼠背部皮下后0 d、1 d、2 d、3 d、5 d和7 d的NIR-II区荧光成像结果。I、II、III、IV分别代表0.5mg/ml,0.1mg/ml,0.05mg/ml外泌体及PbS QDs注射部位(λex: 808 nm,曝光时长: 300 ms)。(b)不同注射位点的荧光面积进行纵向比较。(c)不同注射位点的荧光强度进行纵向比较。(d)0d时注射位点荧光强度与外泌体浓度的线性相关结果

fluorescence signal appeared on the proximal side of the injured femoral nerve, indicating that QDs-ADSC-Exos were injected at the site of femoral nerve injury. Over time, the fluorescence area gradually decreased, reaching 50% at 12 hours and less than 10% at 72 hours (Figure 5c). Fluorescence intensity initially increased within the first 12 hours, followed by a gradual decline, nearly disappearing by 72 hours, indicating that exosomes accumulated at the proximal end of the nerve injury within the first 12 hours and were subsequently metabolized, with signals lasting up to 72 hours (Figure 5(d)). Analysis of the centroid position of NIR fluorescence spots, with the 0 h centroid as the origin, showed that movement toward the proximal end was marked as positive and toward the distal end as negative. Over 72 hours, the centroid remained proximal to the injury site, further demonstrating that in ischemic femoral nerve injury, exosomes primarily accumulate at the proximal end of the nerve injury (Figure 5(e)). These findings indicate that PbS QDs can serve as NIR-II fluorescent probes for labeling ADSC-Exos, enabling the observation of their metabolic characteristics in ischemic peripheral nerve injury. NIR-II imaging of QDs-ADSC-Exos reveals the spatiotemporal distribution of ADSC-Exos in the femoral artery and vein ligation model with femoral nerve injury in rats.

2.3 QDs-ADSC-Exos promote regeneration in ischemic peripheral nerve injury

To assess the role of QDs-ADSC-Exos in nerve regeneration, CMAPs were measured in the quadriceps muscle on day 28 post-injection. The amplitude in the QDs-ADSC-Exos group was (5.17 ± 0.11) mV, significantly higher than the (4.14 ± 0.35) mV observed in the PBS group ($P < 0.01$).

Further evaluation of motor function recovery was performed by measuring FBA and SLR before surgery, and at days 1 and 28 post-injection (Figure 7(a)). The recovery indices for FBA (RI FBA) and SLR (RI SLR) were calculated for day 28. Rats in the QDs-ADSC-Exos group exhibited an RI FBA of 61.25% ± 7.00% and an RI SLR of 43.92% ± 6.00%, whereas the PBS group showed an RI FBA of 78.3% ± 3.51% and an RI SLR of 60.67% ± 4.04%. The QDs-ADSC-Exos group demonstrated significantly better outcomes in both RI FBA and RI SLR compared to the PBS group (Figure 7(b),(c),

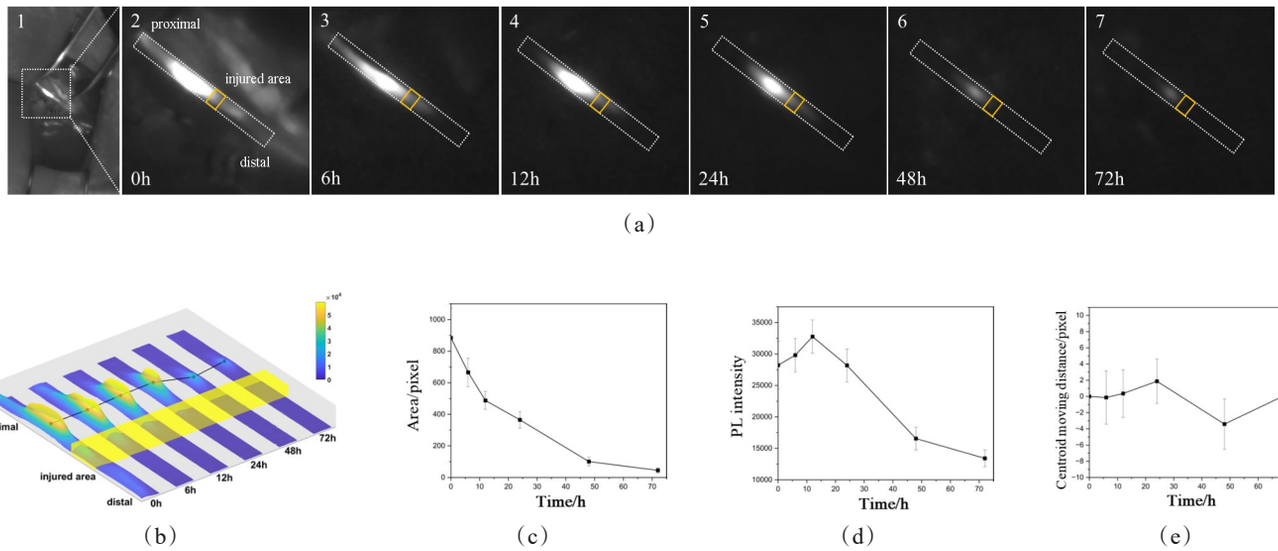

Fig. 5 In vivo monitoring of QDs-ADSC-Exos based on an NIR-II fluorescence imaging strategy in rat models of ischemic femoral nerve injury: (a1-a7) NIR-II fluorescence imaging at various time points (0 h, 6 h, 12 h, 24 h, 48 h, and 72 h) following the injection of 5 μl of 0.5 mg/ml QDs-ADSC-Exos near the proximal region of the femoral nerve in a rat model with femoral artery and vein ligation combined with femoral nerve injury (λex: 808 nm, exposure time: 300 ms); (b) schematic representation of fluorescence signal distribution at different time points, with black dots indicating the fluorescence centroid position and yellow boxes denoting the site of femoral nerve injury; (c) longitudinal comparison of the fluorescence area at different time points; (d) longitudinal comparison of PL intensity at different time points; (e) the centroid positions at different time points were determined, using the centroid position at 0h as the origin. The distances of centroid movement at 0h, 6h, 12h, 24h, 48h, and 72h were then calculated

图 5 近红外二区成像下 QDs-ADSC-Exos 在大鼠伴缺血股神经损伤中的体内动态监测:(a1-a7)5 ul 0.5 mg/ml QDs-ADSC-Exos 注射于伴缺血股神经损伤大鼠股神经近端后 0 h、6 h、12 h、24 h、48 h 和 72 h 的 NIR-II 区荧光成像结果。(λex:808 nm,曝光时长:300 ms);(b)不同时间节点 NIR-II 区荧光信号分布示意,黑点表示荧光光斑质心位置,黄框表示股神经损伤部位;(c)不同时间节点荧光面积的纵向比较;(d)不同时间节点荧光强度进行纵向比较;(d)不同时间节点质心位置,并以 0 h 质心位置为原点,计算 0 h、6 h、12 h、24 h、48 h 和 72 h 质心移动距离

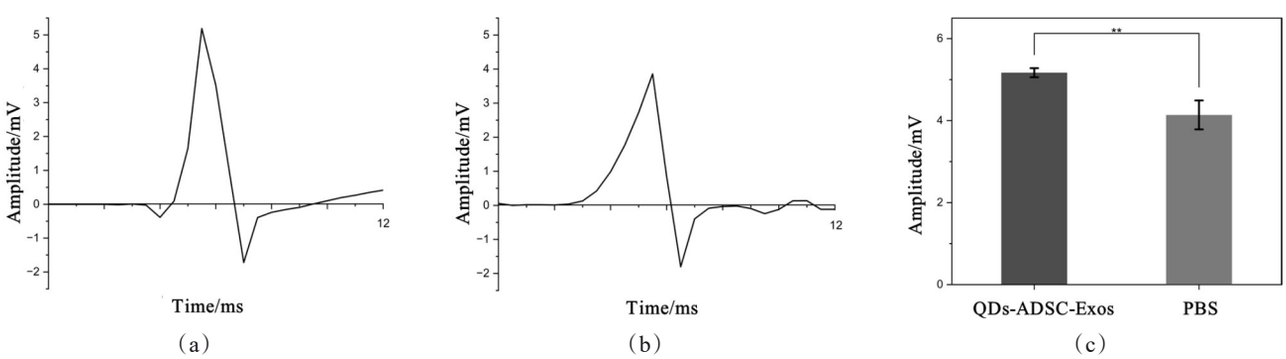

Fig. 6 CMAP of quadriceps muscle measured by electromyography: (a) rats with QDs-ADSC-Exos and (b) PBS injection at 28d post-injection; (c) histogram of signal intensity measured from (a) - (b)

图 6 股四头肌 CMAP 测量结果:(a)注射 QDs-ADSC-Exos 及(b)PBS 28 天后大鼠;(c) (a-b) 中测得信号强度统计直方图

$P < 0.01$), indicating that QDs-ADSC-Exos promote regeneration of the ischemic femoral nerve, enhancing the reinnervation of the quadriceps muscle.

2.4 Biocompatibility and Safety of QDs-ADSC-Exos

To assess the biocompatibility of QDs-ADSC-Exos, rats were sacrificed on day 28, and major organs, including the heart, liver, spleen, lungs, and kidneys, were harvested for NIR-II imaging and HE staining. As shown in Fig. 8(b), the kidney exhibited higher fluorescence intensity than other organs ($P < 0.001$), suggesting renal metabolism of the labeled exosomes. No significant inflammation or other pathological changes were observed in the HE-stained sections of these organs (Figure 8(d)), confirming that QDs-ADSC-Exos possess good biocompatibility and safety.

3 Discussion

Peripheral nerves are supplied by intrinsic and ex-

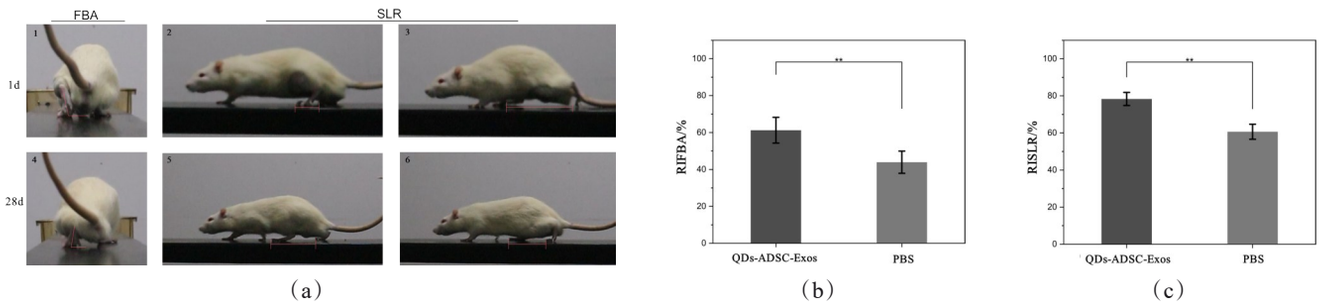

Fig. 7 Postoperative gait analysis in the rat model of ischemia femoral nerve injury: (a1) foot angle relative to the track during movement, (a2) ipsilateral step length, and (a3) contralateral step length at 1 day post-injury; (a4) foot angle relative to the track during movement, (a5) ipsilateral step length, and (a6) contralateral step length at 28 days post-injury. (b) RI FBA and (c) RI SLR comparisons between the QDs-ADSC-Exos and PBS groups at 28 days

图 7 大鼠伴缺血股神经损伤模型的术后步态分析：损伤后 1 天(a1)大鼠爬行足底相对跑道角度，(a2) 患侧步幅及(a3)健侧步幅；损伤后 28 天(a4) 大鼠爬行足底相对跑道角度，(a5)患侧步幅及(a6)健侧步幅于；QDs-ADSC-Exos 组与 PBS 组在术后 28 天(b)RI FBA 及(c)RI SLR 比较

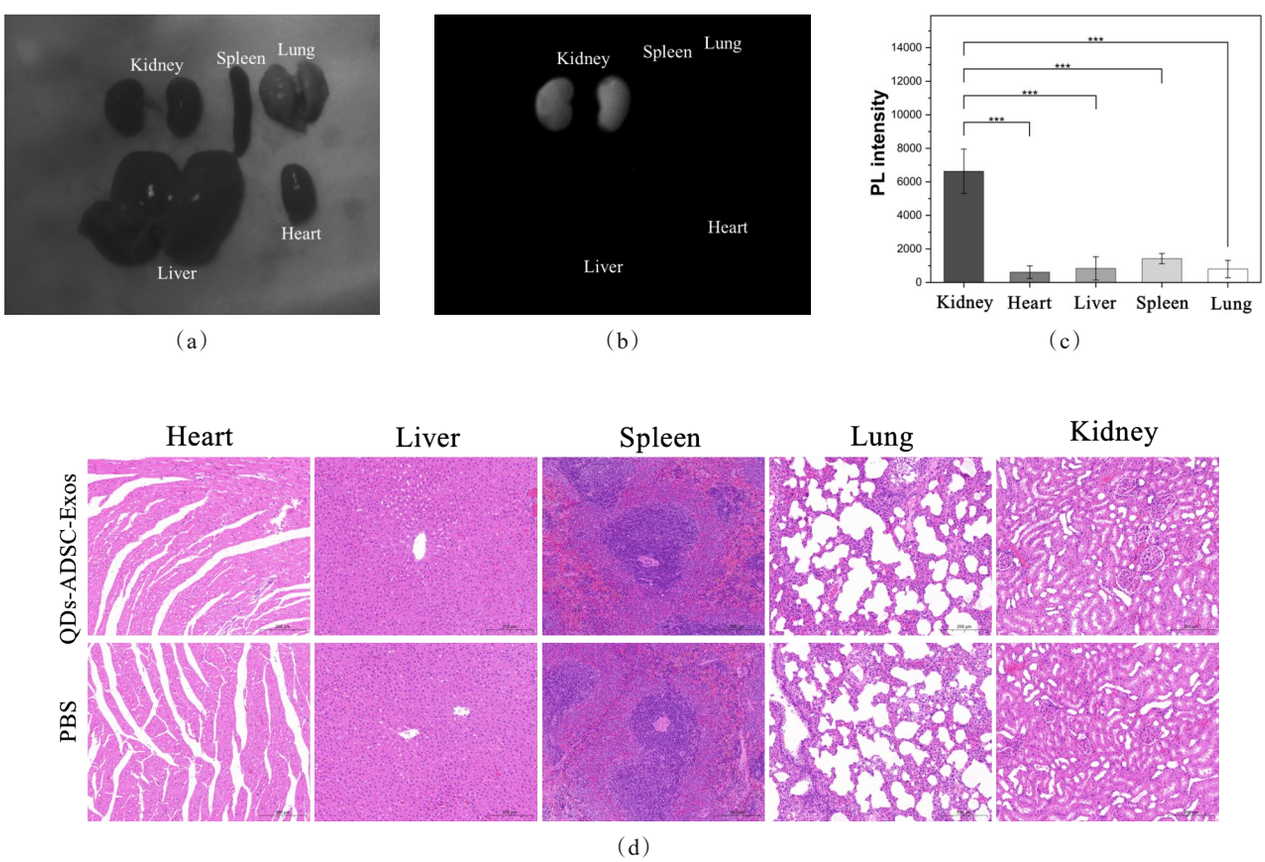

Fig. 8 Biocompatibility and Safety of QDs-ADSC-Exos: (a) bright field photograph and (b) NIR-II fluorescence image of the major organs harvested from the rats 28 days post-injection of QDs-ADSC-Exos; (c) quantification of NIR-II fluorescence signals from the organs shown in (b); (d) histological analysis with H&E staining of the major organs harvested from the the rats in the QDs-ADSC-Exos group and the PBS group at 28 days post-injection (scale bar = 100 μm).

图 8 QDs-ADSC-Exos 生物相容性和安全性检测：(a) 注射 QDs-ADSC-Exos 大鼠主要脏器明场及(b) NIR-II 区荧光图像；(c)主要脏器 NIR-II 区荧光信号定量；(d) 注射后 28 天，QDs-ADSC-Exos 组和 PBS 组主要脏器 HE 染色组织学分析 (比例尺 = 100 μm)。

trinsic vascular networks that ensure metabolic activity. The intrinsic network consists of longitudinally distributed arteries and veins, while the extrinsic network originates from large adjacent vessels, connecting to the intrinsic system via spiral vessels, allowing for nerve movement and extension[17]. This complex vascular network allows the nerve to maintain function even when some vessels are damaged. However, its compensatory ability has

a limit, and extensive vascular destruction can still result in ischemia.

Ischemia triggers necrosis, macrophage activation, and upregulation of endothelial adhesion factors, leading to a pro-inflammatory microenvironment, which is a significant factor hindering complete nerve regeneration[18]. MSC-derived exosomes carry various proteins, miRNAs, and mRNAs that facilitate axonal regeneration, myelin debris clearance, neuronal protection, and immune modulation during peripheral nerve injury[19]. Studies have shown that ADSC-Exos can promote angiogenesis and exert anti-inflammatory effects via miRNA regulation[20]. This study further explores the metabolic characteristics of ADSC-Exos and their role in promoting nerve regeneration in ischemic peripheral nerve injury.

Previous studies on exosomes mainly relied on in vitro cellular experiments and ex vivo tissue sections, providing limited understanding of the real-time spatiotemporal distribution of exosomes in vivo. Research indicates that glucose-modified nanoparticles can be labeled on exosomes through the active transport function of glucose transporter 1 (Glut-1) on the exosome surface[21]. In this study, glucose-modified PbS QD-labeled exosome complexes were successfully constructed, enabling real-time, long-term in vivo imaging through NIR-II technology. The findings indicate that QDs-Glu can noninvasively label ADSC-Exos, maintaining their morphology and function. In vivo imaging showed stable imaging for over 7 days with high clarity and signal-to-noise ratio, and the fluorescence intensity correlated with exosome concentration. NIR-II imaging results of QDs-ADSC-Exos in the femoral artery and vein ligation model with femoral nerve injury indicate that ADSC-Exos accumulate at the proximal end of the nerve injury in ischemic peripheral nerve damage, aligning with previous findings showing that exosomes aggregate at injury sites during tissue repair[22]. Notably, in cases of isolated nerve injury, exosomes are capable of migrating from the proximal end of the injury, crossing the damaged region, and moving distally[23]. However, in ischemic nerve injuries, exosomes consistently accumulate at the proximal end of the nerve injury, potentially due to the relatively static metabolic environment of the nerve in ischemic conditions, which may facilitate the localized retention of exosomes. Electrophysiological and behavioral assessments confirmed the nerve regeneration-promoting effect of ADSC-Exos, along with good biocompatibility.

While this study provides robust evidence for the therapeutic applications of ADSC-Exos in ischemic peripheral nerve injury, certain limitations should be addressed. For instance, NIR-II imaging, while providing superior tissue penetration and reduced autofluorescence, is currently unable to achieve cellular-level resolution or identify exosome localization within specific cell types. Further advancements in imaging technologies may be required to address these challenges. Additionally, modifications to the exosome-labeling process will be essential for clinical translation, including the development of scalable production protocols and compliance with clinical-grade standards for therapeutic applications.

In conclusion, ADSC-Exos facilitate the regeneration of ischemic peripheral nerve injuries, with PbS QDs serving as NIR-II fluorescent probes for real-time, precise imaging of ADSC-Exos in vivo. This study provides direct imaging support for the therapeutic applications of exsomes in ischemic peripheral nerve injury, offering new evidence for their clinical use.

References

[1] Lopes B, Sousa P, Alvites R, et al. Peripheral nerve injury treatments and advances: one health perspective [J]. International Journal of Molecular Sciences, 2022, 23(2): 918.
[2] Carmeliet P, Tessier-Lavigne M. Common mechanisms of nerve and blood vessel wiring [J]. Nature, 2005, 436(7048): 193-200.
[3] Yeoh S, Warner W S, Merchant S S, et al. Incorporating blood flow in nerve injury and regeneration assessment [J]. Frontiers in Surgery, 2022,9: 862478.
[4] Zhang R C, Du W Q, Zhang J Y, et al. Mesenchymal stem cell treatment for peripheral nerve injury: a narrative review [J]. Neural Regeneration Research, 2021, 16(11): 2170.
[5] Sanchez Rezza A, Kulahci Y, Gorantla V S, et al. Implantable biomaterials for peripheral nerve regeneration-technology trends and translational tribulations [J]. Frontiers in Bioengineering and Biotechnology, 2022, 10: 863969.
[6] Gurung S, Perocheau D, Touramanidou L, et al. The exosome journey: from biogenesis to uptake and intracellular signalling [J]. Cell Communication and Signaling : CCS, 2021, 19(1): 47.
[7] Rahimian S, Najafi H, Webber C A, et al. Advances in exosome-based therapies for the repair of peripheral nerve injuries[J]. Neurochemical Research, 2024, 49(8): 1905-1925.
[8] Supra R, Wilson D R, Agrawal D K. Therapeutic potential of "smart" exosomes in peripheral nerve regeneration [J]. Journal of Biotechnology and Biomedicine, 2023, 6(2): 189-196.
[9] Barile L, Vassalli G. Exosomes: Therapy delivery tools and biomarkers of diseases[J]. Pharmacology & Therapeutics,2017,174: 63-78.
[10] Dong R, Liu Y, Yang Y, et al. MSC-derived exosomes-based therapy for peripheral nerve injury: a novel therapeutic strategy [J]. BioMed Research International, 2019, 2019(1): 6458237.
[11] Chen H, Yang H, Zhang C, et al. Differential responses of transplanted stem cells to diseased environment unveiled by a molecular NIR-II cell tracker[J]. Research, 2021, 2021: 9798580.
[12] Liu X C, Zhang H J, Xu R, et al. A NIR-II quantum dot-assisted dual-color imaging strategy enables simultaneous tracking of two subtypes of extracellular vesicles in vivo [J]. Chemical Engineering Journal, 2024, 492: 152242.
[13] Wang F, Zhong Y, Bruns O, et al. In vivo NIR-II fluorescence imaging for biology and medicine [J]. Nature Photonics, 2024, 18(6): 535-547.
[14] Esteve-Turrillas F A, Abad-Fuentes A. Applications of quantum dots as probes in immunosensing of small-sized analytes [J]. Biosensors and Bioelectronics, 2013, 41(1): 12-29.
[15] Kong Y, Chen J, Fang H, et al. Highly fluorescent ribonuclease-a-encapsulated lead sulfide quantum dots for ultrasensitive fluorescence in vivo imaging in the second near-infrared window[J]. Chemistry of Materials, 2016, 28(9): 3041-3050.
[16] Kruspe M, Thieme H, Guntinas-Lichius O, et al. Motoneuron regeneration accuracy and recovery of gait after femoral nerve injuries in rats [J]. Neuroscience, 2014, 280: 73-87.
[17] Yeoh S, Warner W S, Merchant S S, et al. Incorporating blood flow in nerve injury and regeneration assessment [J]. Frontiers in Surgery, 2022, 9: 862478.
[18] Kawabori M, Yenari M. Inflammatory responses in brain ischemia [J]. Current Medicinal Chemistry, 2015, 22(10): 1258-1277.
[19] Ahmed L A, Al-Massri K F. Exploring the role of mesenchymal stem cell-derived exosomes in diabetic and chemotherapy-induced peripheral neuropathy [J]. Molecular Neurobiology, 2024, 61(8): 5916-5927.
[20] Yang S, Sun Y, Yan C. Recent advances in the use of extracellular vesicles from adipose-derived stem cells for regenerative medical therapeutics [J]. Journal of Nanobiotechnology, 2024, 22(1): 1-28.

[21] Betzer O, Perets N, Angel A, et al. In vivo neuroimaging of exosomes using gold nanoparticles. [J]. ACS Nano, 2017, 11(11): 10883.
[22] Lapchak P A, Boitano P D, De Couto G, et al. Intravenous xenogeneic human cardiosphere-derived cell extracellular vesicles (exosomes) improves behavioral function in small-clot embolized rabbits [J]. Experimental Neurology, 2018, 307: 109-117.
[23] Wang Y, Sheng H, Cong M, et al. Spatio-temporally deciphering peripheral nerve regeneration in vivo after extracellular vesicle therapy under NIR-II fluorescence imaging [J]. Nanoscale, 2023, 15(17): 7991-8005.